Supporting Information

Hierarchical Porous Carbon Aerogel Derived from Bagasse for High Performance Supercapacitor Electrode

Pin Hao‡[a], Zhenhuan Zhao‡[a], Haidong Li[a], Jian Tian[a], Yuanhua Sang[a], Guangwei Yu[a],Huaqiang Cai[b], Hong Liu[a], C. P. Wong[c*], Ahmad Umar[d,e]**

[a] State Key Laboratory of Crystal Materials, Shandong University, Jinan, Shandong 250100, People's Republic of China

[b]Institute of Chemical Materials, China Academy of Physical engineering, Mianyang, 621900, PR China

[c]School of Materials Science and Engineering, Georgia Tech, Atlanta, GA 30032

[d]Department of Chemistry, Faculty of Science and Arts, Najran University, Najran-11001, Kingdom of Saudi Arabia

[e] Promising Centre for Sensors and Electronic Devices (PCSED), Najran University, Najran-11001, Kingdom of Saudi Arabia

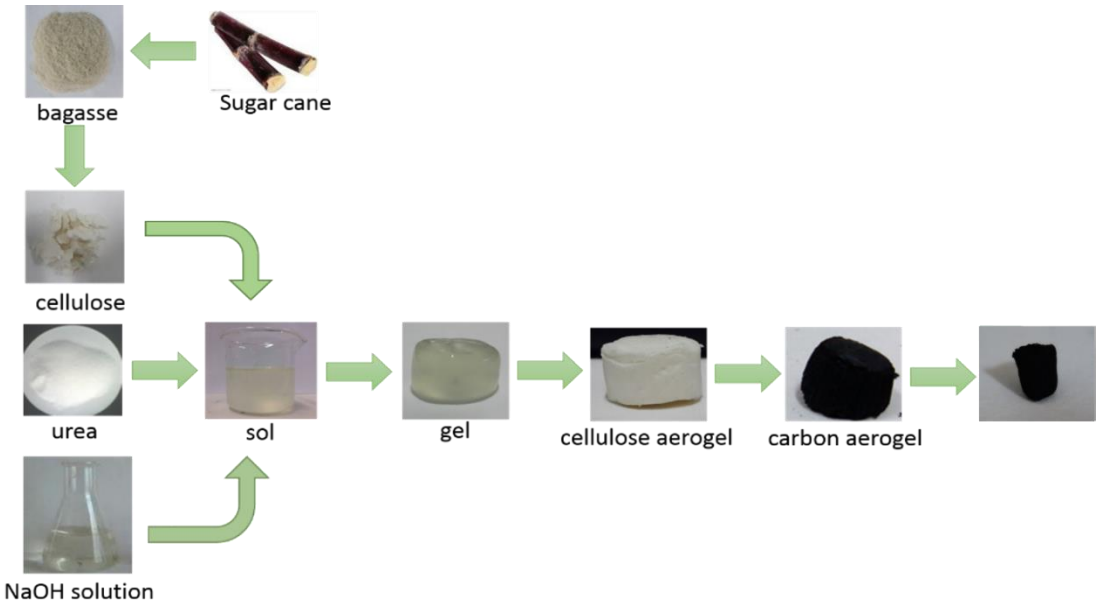

Fig. S1 Photo flow diagram for the fabrication of bagasse-derived carbon aerogels

The photo flow diagram is schematically illustrated in figure S1. The used cellulose fibers were obtained from purification of bagasse. The first step is the dissolution of cellulose fibers, in which the solvent mixture of NaOH/urea/H_2O (7.5:11.5:81w/w) was used. After the regeneration and freeze drying process, the cellulose aerogels can be obtained. Carbon aerogels were obtained after carbonized at 800 °C. To further optimize the pore size distribution and formed a hierarchical porous structure, the obtained carbon aerogels were then activated using KOH solution. The resulting mixture was then washed and dried, yielding a hierarchical porous structure.

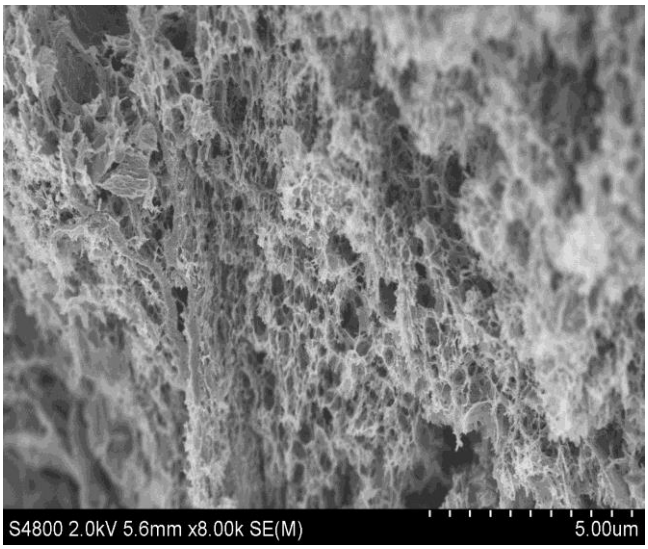

Fig. S2. Typical FESEM image of the cellulose aerogel

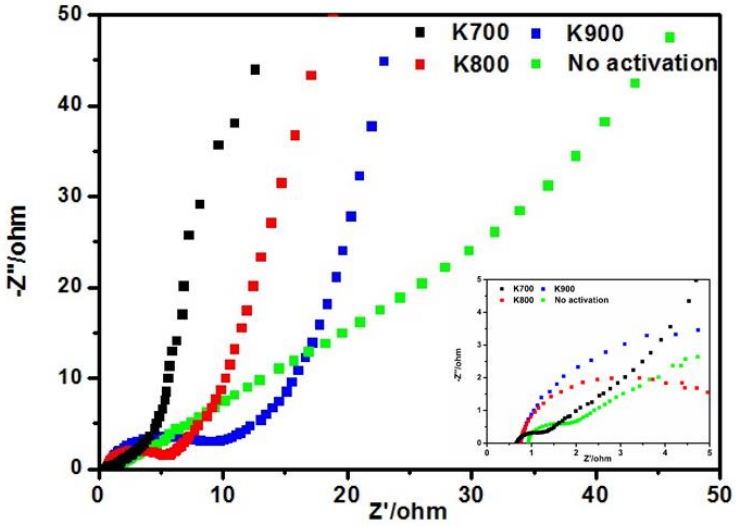

Fig. S3. Nyquist plots showing the imaginary part versus the real part of impedance in 6 M KOH aqueous solution, Inset magnifies the data in the high-frequency range

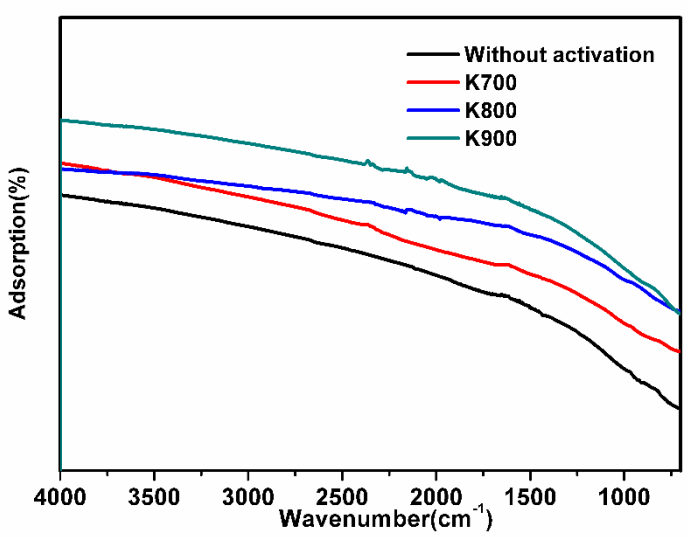

Fig. S4.FTIR spectra of the pristine and activated samples

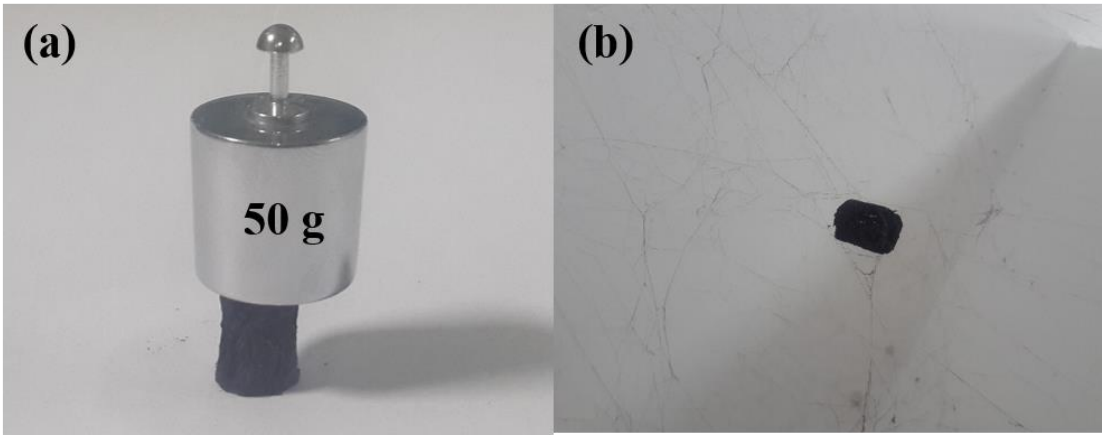

Fig. S5. Photographs of the carbon aerogel (a) supporting a 50 g weight and (b) on the spider web

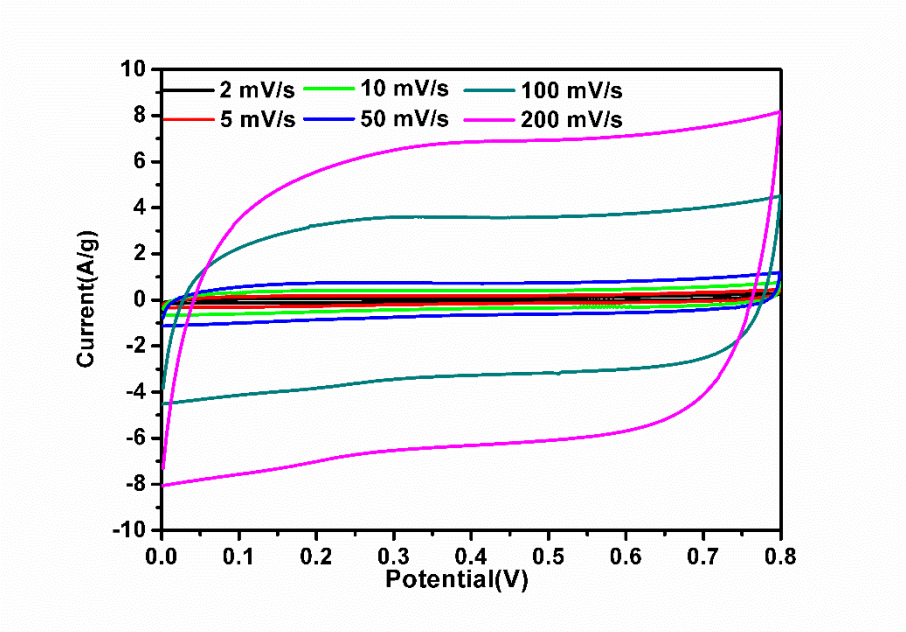

Fig. S6. CV curves of two-electrode symmetrical supercapacitor at varied potential scan rates in liquid electrolyte.

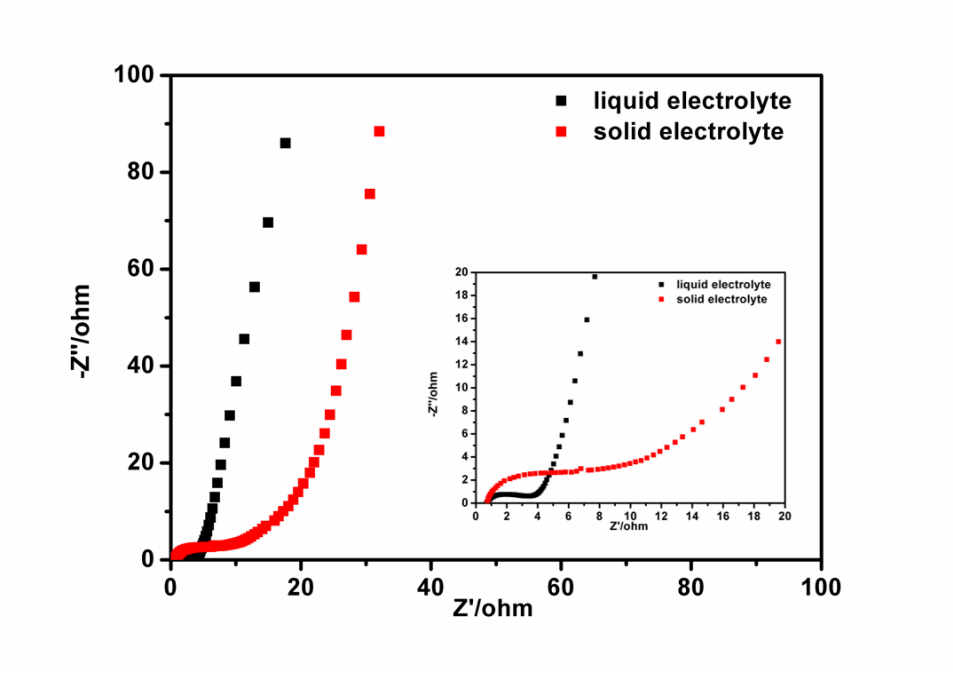

Fig. S7. Nyquist plots showing the imaginary part versus the real part of impedance in liquid and solid electrolyte. Inset magnifies the data in the high-frequency range